

ASSESSMENT OF R290 AS A POSSIBLE ALTERNATIVE TO R22 IN DIRECT EXPANSION SOLAR ASSISTED HEAT PUMPS

by

**Lokesh PARADESHI*, Srinivas MOKKALA,
and Jayaraj SIMON**

Department of Mechanical Engineering,
National Institute of Technology, Calicut, India

Original scientific paper
<https://doi.org/10.2298/TSCI17S2369P>

In this paper, the energy performance of a direct expansion solar assisted heat pump has been experimentally assessed with R290 as an alternative to R22 to meet the requirements of Kigali agreement. The experiments have been performed at Calicut climatic conditions (latitude of 11.15° N, longitude of 75.49° E) during the winter climates of 2016. The performance parameters such as, compressor power consumption, condenser heating capacity, energy performance ratio, and solar energy input ratio were evaluated for energy performance comparison. The results showed that, R290 has 6.8% higher energy performance ratio when compared to R22, with 11% reduction in compressor power consumption. Moreover, R290 has negligible global warming impact and zero ozone depletion potential when compared to R22. The effect of wind speed, collector area, ambient temperature, and solar insolation on the system performance found to be with an average value of 0.85%, 12%, 2.5%, and 4.5% for the selected refrigerants, respectively.

Key words: R290, direct expansion solar assisted heat pumps,
energy performance assessment

Introduction

Heat pumps are recognized as an energy efficient appliance due to its capability to deliver more output heat than work input it takes in [1]. Heat pumps are used for drying, water heating, space heating, and desalination applications. The performance of heat pumps is improved by integrating it with solar energy. During last two decades, many research and development activities have reported on direct expansion solar assisted heat pump (DXSAHP) systems, which are summarized in earlier review articles [2, 3]. The halogenated refrigerant compounds are most widely used in compression based heat pump systems due to its favorable characteristics for heat pump applications [4-6]. The Montreal protocol 1987 has restricted the usage of chlorine based refrigerants in refrigeration, air conditioning, and heat pump systems. Further, Kyoto protocol 1997 has restricted the usage of HFC refrigerants. India has also signed in Paris protocol to reduce to the consumption of HFC refrigerants in refrigeration and air conditioning industries. Many researchers have tried R290 as a possible alternative to R22 in air conditioning and heat pump systems. In a related study, Pukshya and Bansal [7] investigated the performance of a R22 based heat pump working with R290

* Corresponding author, e-mail: lokeshpb@gmail.com

and liquefied petroleum-gas mixture as alternatives and reported with 18% and 12% improved performance, respectively. Further, Chaichana *et al.* [8] theoretically compared the performance of R22 and R290 and reported that R290 is a good substitute to R22. The performance of hydrocarbons such as R290 and R600a was also tested in a commercial heat pump as R22 substitute [9]. The results reported that heating capacity of hydrocarbon refrigerant mixtures increases with increase in mass fraction of R290. Further, the performance of R1270, R290, RE170, and R152a as alternatives to R22 were experimentally investigated in a residential air conditioner [10]. Their results showed that these working fluids have 5.7% higher COP when compared with R22, while propane (R290) showed 11.5% reduction capacity as compared to that of R22. Mohanraj *et al.* [11] compared the performance of a DXSAHP using R22 and a mixture of R407C with liquid petroleum gas. It was reported that the proposed new refrigerant mixture has 1.2% higher power consumption with 1-4.5% reduction in heating capacity when compared to R22. Chata *et al.* [12] proposed a theoretical study on DXSAHP system for sizing of solar collector using different refrigerants. Their results reported that selection of collector size should match the compressor heating capacity for better system performance. However, the thermal response of R290 in a DXSAHP under the influence of fluctuating evaporator-collector loading conditions was not reported in open literature. Hence, an attempt has been made in this work to investigate the energy performance and thermal response of R290 under the influence of fluctuations in solar irradiation and compared against R22.

Characteristics of R290 and R22

The R290 is a hydrocarbon refrigerant with zero ozone depletion potential and negligible global warming potential. The R290 is highly miscible with mineral oil, which is commonly used user friendly lubricant in R22 based compressors.

Table 1. Thermodynamic properties of R22 and R290

Refrigerant	Molecular weight	Temperature [°C]	Pressure [MPa]	Boiling point [°C]
R22	86.47	96.2	4.99	-41.4
R290	44.1	96.7	4.25	-42.1

Thermodynamic properties such as critical pressure, critical temperature, boiling point, and molecular weight of R290 are compared with R22 in tab. 1.

Thermo-physical properties such as vapor pressure and latent heat of R22 and R290 in the temperature range between 0 and 70 °C are compared in fig. 1. From fig. 1, it is confirmed that the vapor pressure of R290 was found to be closer to R22 in the temperature range between 0 and 25 °C. At higher temperatures, the vapor pressure of R290 was found to be lower than R22 by about 10%, which confirms that condenser design is safe at high operating temperatures. It is confirmed that R290 has about 70% higher latent heat, which is capable of absorbing and delivering more heat through the solar collector-evaporators and condensers across the wide range of operating temperatures. Similarly liquid density and compressor ratio of R22 and R290 in the temperature range between 0 and 70 °C are compared in fig. 2.

The assessment of the DXSAHP system found to be based on the amount of refrigerant charged in the system that depends on the density of the liquid. The R290 has 58% lower density (average value) compared to R22 for the given operating temperature range. Hence the required charge of the new alternative refrigerant R290 would be less as compared R22. The compressor pressure ratio the R290 is less as compared to R22. Lower compression ratio results in lower power consumption and high volumetric efficiency, higher the system performance.

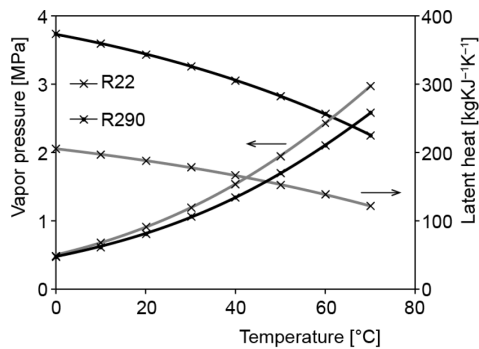


Figure 1. Vapor pressure and latent heat of R22 and R290

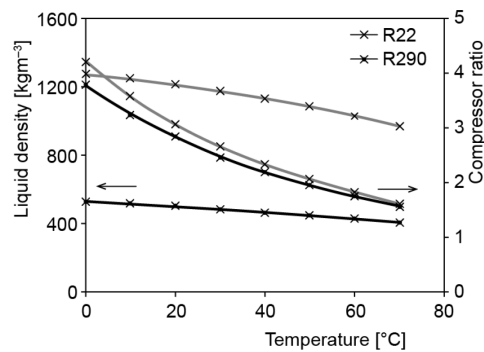


Figure 2. Liquid density and compression ratio of R22 and R290

Experimental set-up

Experiments were carried under the meteorological conditions of Calicut city (latitude of 11.15° N, longitude of 75.49° E) in India during the year 2016.

Experimental set-up

The schematic diagram of a DXSAHP is illustrated in fig. 3 and its technical specifications are listed in tab. 2. The DXSAHP consists of R22 based reciprocating compressor, air cooled condenser, thermostatic expansion valve and glazed evaporator – solar collector of 2 m² collecting area to absorb 2.8 kW of heat from solar as well as ambient. In addition, the accessories such as, liquid receiver, refrigerant drier, and sight glass were installed in liquid line. The evaporator-collector consists of 0.8 mm copper fins with 10 mm length attached with copper tubes. The absorber plate is coated with black paint to increase the heat absorption. The absorber plate along with copper tube was placed behind the glass cover by maintaining 50 mm air gap to produce greenhouse effect. Bottom side of the absorber plate was insulated with 25 mm glass wool insulation to reduce the heat loss at the bottom side of the collector. The collector was placed at an angle of 20° inclination by facing south to maximizing the absorption of solar irradiation.

Table 2. Specifications of components used in experimental set-up

Component	Specification
Compressor	Hermetically sealed type Power input: 1020 W Cooling capacity: 2750 W Rated speed: 2800 rpm
Condenser	Air cooled type; air flow 4.75 m/s
Collector	Type: flat plate collector; area: 2 m ²
Expansion valve	Thermostatic expansion type
Refrigerant(s)	R290 and R22

Instrumentation

Temperature and pressure of refrigerant at typical locations in DXSAHP circuit are measured using PT 100 sensors and Bourdon tube pressure gauges. In addition, the pressure values are also measured using pressure transducers installed at salient location in DXSAHP circuit as illustrated in fig. 3. The air temperatures at condenser inlet and outlet are also measured using PT 100 temperature sensors. All the temperature sensors and pressure transducers

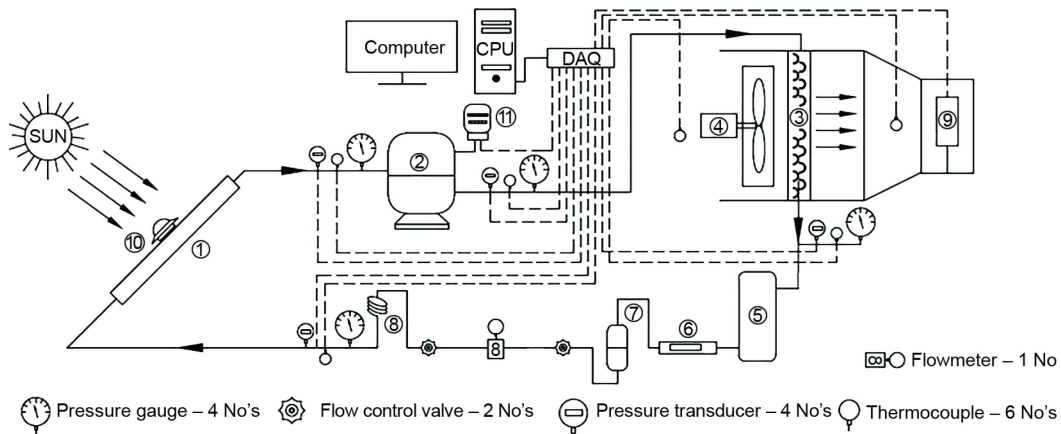


Figure 3. Schematic diagram of a DXSAHP system; 1 – solar collector, 2 – compressor, 3 – air cooled condenser, 4 – condenser fan, 5 – liquid receiver, 6 – sight glass, 7 – refrigerant dryer, 8 – thermostatic valve, 9 – anemometer, 10 – pyranometer, 11 – digital wattmeter

Table 3. Specifications of the instruments

Instrumentation	Specification/range	Accuracy
Temperature sensor	PT 100/0-200 °C	±0.1 °C
Pressure sensor	HAE-24/0-24 bar	±0.01 bar
Thermometer	0-100 °C	±0.5 °C
Anemometer	Vane type	±0.1 m/s
Pyranometer	Class A/0-1500	±5 W/m ²
Wattmeter	Digital type	±1 W

and relative humidity were recorded in a weather station. The accuracies of instruments are listed in tab. 3.

Experimental procedure

The system was initially flushed and leak tested with nitrogen gas to remove the impurities inside the system. Air and other non-condensable gas inside the system were removed with the help of vacuum pump. First, the system was charged with 1100 g of R22 (as per the manufacturer recommendation) and also with required quantity of lubricant oil. The system is switched ON and allowed to run for the period of one hour to attain steady-state conditions. Experimental observations were made after one hour to avoid initial transient errors. The temperature and pressure of refrigerant at typical locations in heat pump circuit, air temperature at condenser inlet and outlet, ambient parameters such as, solar irradiation, temperature, wind velocity, and relative humidity were measured every ten minutes between 9.00 and 18.00. More data observations were made to investigate the transient behavior of the system and also to eliminate the erroneous data in the observation. After completion of baseline tests with R22, the refrigerant was recovered from the system and charged with equivalent quantity of R290 was charged. The equivalent quantity of R290 was identified based on liquid density

were interfaced with the computer with the help of data logger. For measurements of the instantaneous compressor power consumption and energy consumption per day wattmeter and energy meters were used, respectively. The ambient parameters such as solar irradiation, temperature, wind velocity,

values obtained from REFPROP[®] database. The experimental procedure was repeated for R290 and the performance observations were recorded.

Uncertainty analysis

The uncertainties in experiments are calculated:

$$u_f = \sqrt{\left(\frac{\partial f}{\partial x_1} u_{x_1}\right)^2 + \left(\frac{\partial f}{\partial x_2} u_{x_2}\right)^2 + \dots + \left(\frac{\partial f}{\partial x_n} u_{x_n}\right)^2} \quad (1)$$

The uncertainties in compressor power consumption, condenser heating capacity, energy performance ratio, and solar energy input ratio are calculated as ± 1.14 , ± 2.4 , ± 2.8 , and $\pm 1.8\%$, respectively.

Modeling of DXSAHP system

The thermodynamic analysis of a DXSAHP system was carried out by developing the system simulation model. The system simulation model is consisting of basic governing equation of individual components with these assumptions. All the processes are steady-state, refrigerant mass flow rate is constant, compression and expansion of refrigerant are considered to be polytrophic and isenthalpic process, respectively.

Compressor

The cooling capacity and power consumption of a compressor are represented in terms of their evaporating and condensing temperature. The selected compressor was characterized based on experimental data and expressed:

$$P = -141177.4137 - 2109.6034t_c - 71.6690t_c^2 + 730.0572110t_c - 8.7795t_c^2 - 103.4353t_e t_c - 3.5528t_e^2 t_c + 1.22629t_e^2 t_c - 0.0435t_e^2 t_c^2 \quad (2)$$

$$q_e = -162952.06 + 24211.50t_e - 858.13t_e^2 + 8679.0371t_e - 113.48t_e^2 - 1292.0230t_e t_c + 46.0235t_e^2 t_c + 16.9747t_e^2 t_c - 0.6044t_e^2 t_c^2 \quad (3)$$

Condenser

Heating capacity of condenser is defined as the useful heat delivered at the condenser exit. It is the sum of useful heat gained at evaporator/solar collector and energy input to the compressor. Condenser modelling is given by:

$$q_c = \dot{m}_{\text{air}} C_{pa} (t_c - t_{\text{amb}}) \quad (4)$$

Solar collector/evaporator

The heat absorbed by the glazed type solar collector/evaporator during the operation can be expressed:

$$q_e = A_c F' [\alpha S - U_o (t_e - t_{\text{amb}})] \quad (5)$$

Assuming the perfect contact between the absorber plate and tube, collector efficiency factor (F') in eq. (5) is given by:

$$F' = F + (1 - F) \frac{D}{W} \quad (6)$$

Similarly, fin efficiency, F , can be calculated using the correlation:

$$F = \frac{\tanh \sqrt{\frac{U_o}{\lambda_p \delta_p} \frac{W - D}{2}}}{\sqrt{\frac{U_o}{\lambda_p \delta_p} \frac{W - D}{2}}} \quad (7)$$

The overall heat transfer coefficient, U_o , is given by:

$$U_o = U_t' + \frac{k_{in}}{x} + \frac{k_{in}}{x} 0.5 \quad (8)$$

The top heat loss coefficient factor is calculated by:

$$U_t' = h_{top} + h_{rad} \quad (9)$$

where h_{top} is the convective heat transfer coefficient at top glass cover generally calculated using eq. (10). The radiation heat transfer coefficient, h_{rad} , has been neglected.

$$h_{top} = 5.7 + 3.8u_w \quad (10)$$

System performance

The energy performance of a DXSAHP system is defined in terms of energy performance ratio (EPR). The EPR is the ratio of condenser heating capacity to the power input of the compressor:

$$EPR = \frac{q_c}{P} \quad (11)$$

The individual component modelling of a DXSAHP system is discussed in previous section. The achieved expressions/modelling equations are solved in MATLAB (Version 9.1) using Newton-Raphson method.

Results and discussions

The energy performance of a DXSAHP system is compared working with R22 and R290. The experiments were carried out during winter season of 2016. The experimental observations, thermal performance parameters such as power consumption, heating capacity, energy performance ratio, and solar energy input ratio are discussed in this section.

Variation of ambient conditions

The results obtained from series of experimental observations in a DXSAHP using R22 and R290 are compared. Continuous experimental observations are made in a DXSAHP working with R22 and R290 for the period of four months. However, the similar ambient variations observed on January 23 and March 23 were considered for discussions. Variations of solar insolation and ambient temperature against time of the day for selected dates are shown

in fig. 4. The solar insolation is varies from 98 to 938 W/m^2 . For both selected days with an average insolation of 455 W/m^2 during the experimentation. But the average eight hours potential sunshine hours were available during the experimentation. The maximum fluctuation of solar variation is observed to be 40 W/m^2 . Similarly, the variation of ambient temperature during the experimentation observed that, it is various from 28.5 to 35.7 $^{\circ}C$ with an average ambient temperature of about 31.5 $^{\circ}C$. The higher ambient temperature for flat plate collector (glazed type) helps reduces the convection losses also increases in system performance. The variation of wind speed during the experimentation was recorded at regular interval of time. This will enhance in the evaporating temperature of the working fluid and consequently increases hence the system performance. The wind velocity was varied in the range between 0.5 m/s and 4.5 m/s with an average value of 1.5 m/s.

Performance of compressor and condenser

The experimentally measured performance parameters were well agreed with simulation results with an average error about 1-2%. The variation in compressor power consumption and condenser heating capacity during the experimentation is depicted in fig. 5. The compressor power consumption was varied from 961 to 1172 W and 1092 to 1310 W for R290 and R22, respectively. The power consumption of compressor for R290 is about 11% lower than that of R22, due to its lower vapor pressure and hence increases in system performance. Similarly, the condenser heating capacity of a DXSAHP of R290 and R22 experimental and simulation results are compared. The working fluid temperature at the exit of condenser and outlet air temperature found to be lower during the experimentation for R290. This is due to lower vapor pressure of R290. Hence condenser heating capacity will be lower for R290 with an average value of 5.8% compared to R22. R290 is good alternative choice for R22 in terms of compressor power consumption.

Energy performance ratio and solar energy input ratio

The overall performance of the DXSAHP system is measured in with help energy performance ratio (EPR). Energy performance ratio is nothing but the ratio condenser output

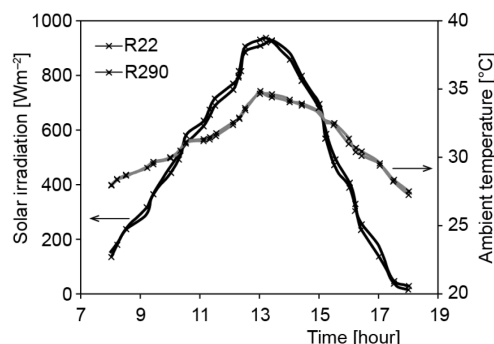


Figure 4. Variation of solar irradiation and ambient temperature

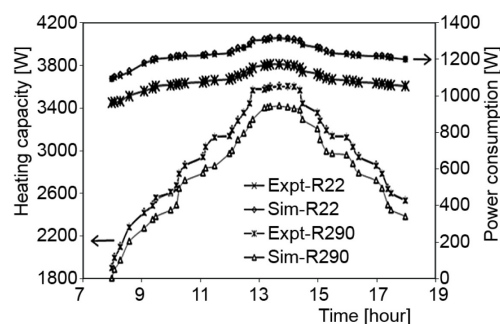


Figure 5. Variation of heating capacity and power consumption

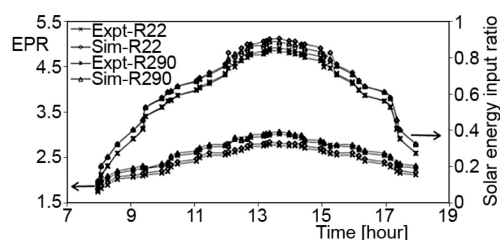


Figure 6. Variation of EPR and SEIR

to the power input to the compressor. The energy performance ratio of a DXSAHP system working with R22 and R290 is depicted in fig. 6. It is observed that system performance varies from 1.87 to 2.99 for R290 and 1.73 to 2.76 for R22, respectively. The maximum system performance is observed during 13.30 h. A maximum solar insolation of around 938 W/m^2 was observed around 13.00 h whereas working fluid attained maximum evaporating temperature during 13.30 h. The maximum energy performance ratio for the both working fluids has been attained when the evaporating temperature attained maximum value. The EPR results indicate that R290 is a suitable working fluid for DXSAHP system for alternative to R22. The solar energy input ratio (SEIR) is another important parameter considered for evaluating the performance of the solar collector used. The SEIR of R290 is found to be little higher than that of R22 in the range of 7-15% due to its higher latent at low evaporating temperatures. For the refrigerants investigated the average SEIR values are found to be in the range of 65-70%. This indicates that remaining heat is absorbed from the ambient source and the temperature difference between absorber surface and temperature of air in the gap between absorber and glazing surface.

Parameteric analysis

The influence of wind speed, ambient temperature, collector area, and solar intensity are illustrated in figs. 7-10. From fig. 7, it is observed that the influence of wind speed at fixed collector area of 2 m^2 , $30 \text{ }^\circ\text{C}$ ambient temperature and solar irradiation of 550 W/m^2 , has minor influence on EPR of DXSAHP working using R22 and R290. Similarly, the influence of ambient temperature is shown in fig. 8. It is observed that, the EPR was increased from 2.2 to 2.5 and from 2.3 to 2.7 for R22 and R290, respectively, under the influence of increase in ambient temperature from 22 to $38 \text{ }^\circ\text{C}$. In fig. 9, the influence of collector area on EPR of DXSAHP is illustrated. It is confirmed that the EPR was increased from 1.3 to 2.7 and from 1.4 to 2.9 for the refrigerants R22 and R290, respectively, under the influence of collector area changing from 0.5 m^2 to 3.5 m^2 . The effect of solar irradiation on EPR is shown in fig. 10. It is observed that, the EPR was increased from 1.7 to 2.5 and from 1.8 to 2.7 with increase in solar irradiation

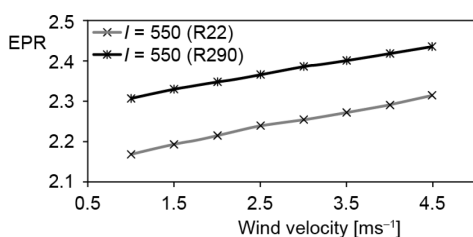


Figure 7. Effect of wind speed

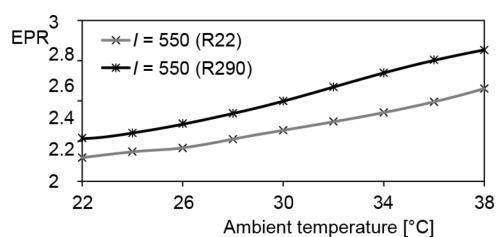


Figure 8. Effect of ambient temperature

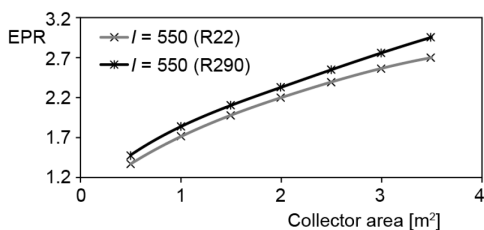


Figure 9. Effect of collector area

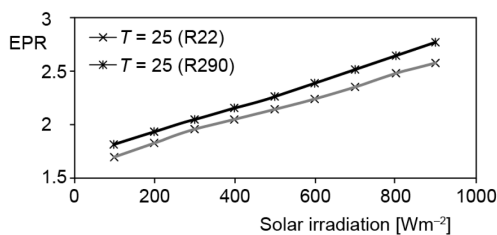


Figure 10. Effect of solar irradiation

from 100 W/m^2 to 900 W/m^2 with collector area of 2 m^2 , ambient temperature of $30 \text{ }^\circ\text{C}$ and, wind velocity of 2.5 m/s . The results confirmed that ambient temperature, collector area, and solar irradiation have significantly influenced the performance of DXSAHP.

Conclusions

The following conclusions are made based in this study.

- The simulation results are closer to the experimental results with maximum deviations of 2%.
- The compressor power consumption and heating capacity for R290 found to be lower about 11% and 5.4%, respectively, when compared to R22.
- The energy performance ratio of R290 is about 6.8% higher compared to R22.
- An improved compressor life is expected using R290 due to its lower compressor discharge temperature compared to R22.
- The influence of wind speed, collector area, ambient temperature, and solar insolation on the system performance are found to be on an average value of 0.85, 12, 2.5, and 4.5% for the selected refrigerants, respectively.

The results confirmed that use of R290 in DXSAHP is an environment friendly and energy efficiency option to phase out R22 in heat pump applications.

Nomenclature

A_c – evaporator/solar collector area, [m^2]

C_{pa} – specific heat of air, [$\text{kJkg}^{-1}\text{K}^{-1}$]

D – diameter of the tube, [m]

k_{in} – thermal conductivity of insulation, [$\text{Wm}^{-1}\text{K}^{-1}$]

\dot{m}_{air} – mass flow rate, [kgs^{-1}]

P – power consumed by the compressor, [W]

q_c – heat rejected at condenser, [W]

q_e – heat absorbed by the solar collector/evaporator, [W]

S – total solar insolation, [Wm^{-2}]

t – temperature, [$^\circ\text{C}$]

W – width of the tube, [m]

u_w – wind speed, [ms^{-1}]

Greek symbols

α – absorptivity of plate material

δ_p – thickness of plate material, [m]

λ_p – thermal conductivity of plate [$\text{Wm}^{-1}\text{K}^{-1}$]

Subscripts

amb – ambient

c – condenser

e – evaporator

t' – top

References

- [1] Mohanraj, M., et al., Performance of a Direct Expansion Solar Assisted Heat Pump Using Artificial Neural Networks, *Applied Energy*, 86 (2009), 9, pp. 1442-1449
- [2] Hawlader, M. N. A., et al., Solar Heat Pump Drier and Water Heater, *Applied Energy*, 74 (2003), 1-2, pp. 185-193
- [3] Chu, J., Cruickshank, C. A., Solar Assisted Heat Pump Systems: A review of Existing Studies and Their Applicability to Canadian Residential Sectors, *Journal of Solar Energy Engineering*, 136 (2014), 4, ID SOL-13-126
- [4] Ni, L., et al., A Review of Heat Pump Systems for Heating and Cooling of Buildings in China in the Last Decade, *Renewable Energy*, 84 (2015), 1, pp. 30-45
- [5] Mohanraj, M., et al., Environment Friendly Alternatives to Halogenated Refrigerants – A Review, *International Journal Green House Gas Emission and Control*, 3 (2009), 1, 108-119
- [6] Yang, Z., Wu, X., Retrofits and Options for the Alternatives to HCFC22, *Energy*, 59 (2013), 1, pp. 1-23
- [7] Bansal, P., Purkayastha, B., An Experimental Study on HC290 and a Commercial Liquefied Petroleum Gas (LPG) Mix as Suitable Replacements for HCFC22, *International Journal of Refrigeration*, 21 (1998), 1, pp. 3-17
- [8] Chaichana, C., et al., Natural Working Fluids for Solar Boosted Heat Pumps, *International Journal of Refrigeration*, 26 (2003), 6, pp. 637-643

- [9] Chang, Y. S., et al., Performance and Heat Transfer Characteristics of Hydrocarbon Refrigerants in a Heat Pump System, *International Journal of Refrigeration*, 23 (2000), 3, pp. 232-242
- [10] Park, K.-J., et al., Performance of Alternative Refrigerants for Residential Air Conditioning Applications, *Applied Energy*, 84 (2007), 10, pp. 985-991
- [11] Mohanraj, M., et al., A Comparison of the Performance of a Direct Expansion Solar Assisted Heat Pump Working with R22 and a Mixture of R407C – Liquefied Petroleum Gas, *Proceedings of the Institution of Mechanical Engineers, Part A: Journal of Power and Energy*, 223 (2009) 7, pp. 821-833
- [12] Chata, G. F. B., et al., Analysis of a Direct Expansion Solar Assisted Heat Pump Using Different Refrigerants, *Energy Conversion and Management*, 46 (2005), 15-16, pp. 2614-2624